Three-Coordinate Thiolato Complexes of Zinc: Solution and Solid-State Structures and EHMO Analysis of the Bonding Pattern of $[Zn(S\text{-}t\text{-}Bu_3C_6H_2\text{-}2,4,6)_2]_2$

Manfred Bochmann,* Gabriel Bwembya, Roger Grinter,* Jianjun Lu, Kevin J. Webb, and David J. Williamson

School of Chemical Sciences, University of East Anglia, Norwich NR4 7TJ, U.K.

Michael B. Hursthouse and Muhammed Mazid

School of Chemistry and Applied Chemistry, University of Wales, P.O. Box 912, Cardiff CF1 3TB, U.K.

Received May 19, 1992

The volatile zinc thiolato complex $Zn(SAr'')_2$ (**1**) ($Ar'' = C_6H_2\text{-}t\text{-}Bu_3\text{-}2,4,6$) was characterized by variable-temperature and solid-state ^{13}C CP-MAS NMR and X-ray crystallography. The compound is dimeric in the solid state, with trigonal-planar zinc coordinated to three sulfur ligands and asymmetric thiolato bridges. In benzene solution, **1** dissociates into two-coordinate monomers, while at low temperature dimeric species exist in dichloromethane or toluene. The skeletal bonding pattern and the asymmetry of the thiolato bridges are explained on the basis of EHMO calculations; the Zn–S bonds are essentially σ in character, with negligible contributions from Zn–S $(p\text{–}p)_\pi$ interactions. Crystal data for **1**: triclinic space group $P\bar{1}$; $Z = 2$; $a = 10.333(5)$, $b = 11.226(9)$, $c = 32.266(30)$ Å; $\alpha = 81.29(2)$, $\beta = 86.12(2)$, $\gamma = 86.07(2)°$; $V = 3684.70$ Å^3; $R = 0.059$, $R_g = 0.068$ based on 4519 reflections with $F_o \geq 2\sigma(F_o)$.

Introduction

Neutral thiolato complexes of zinc and cadmium $[M(SR)_2]_n$ form in general infinite lattices with bridging ligands and tetrahedrally coordinated metal centers.[1] The degree of association and the structural type are sensitive to the steric requirements of the substituent R. As part of our search for new single-source precursors for II–VI semiconducting materials,[2-6] we have recently employed the sterically highly hindered ligands $2,4,6\text{-}t\text{-}Bu_3C_6H_2E^-$ ($AR''E^-$; E = S, Se, Te) and isolated volatile nonpolymeric chalcogenolato complexes which are dimeric in the solid state, with three-coordinate metal centers, and possess sufficient volatility to allow the deposition of II–VI films from the gas phase.[5] The dimeric nature of the cadmium complexes $Cd(EAr'')_2$ (E = S, Se) in the solid state was confirmed by X-ray diffraction, while NMR evidence suggested the existence of monomers in solution.[2,3] For analogous zinc complexes, the evidence was less conclusive. For example, the infrared spectrum of $Zn(SAr'')_2$ (**1**) shows a single strong ν(M–S) band at 390 cm^{-1} and strongly resembles the spectrum of monomeric $Hg(SAr'')_2$ (ν_{asym}(M–S) 378 cm^{-1}),[6] and it could be argued that in the case of zinc, with its small ionic radius of 0.74 Å, compared to 0.97 Å for cadmium(2+),[7] the steric hindrance of the thiolato ligands is sufficient to preserve a monomeric structure in the solid state. The existence of two-coordinate monomers in solution is supported by the recent structure determination of a simple 1:1 diethyl ether adduct $Zn(SAr'')_2(Et_2O)$ by Power et al., who also speculated that **1** might be monomeric in the solid state.[8] On the other hand, ketones and aldehydes react with **1** to give four-coordinate complexes,[9] and with related bulky thiolate ligands three- and four-coordinate complex anions have been characterized.[10] Clearly, further investigations were required to elucidate the structure of **1** in solution and in the solid state, and we report here the results of NMR and X-ray diffraction studies and suggest an explanation of the main structural features based on EHMO calculations.

Experimental Section

General Procedures. All reactions were carried out under argon using standard vacuum-line techniques. Solvents were distilled under nitrogen from sodium–benzophenone (diethyl ether, THF, petroleum ether), sodium (toluene), or calcium hydride (dichloromethane). NMR solvents were stored over 4A molecular sieves and degassed by freeze–thaw cycles. Solution NMR spectra were recorded using JEOL EX90Q and GX400 instruments, and solid-state NMR spectra were recorded at 50.29 MHz using an instrument built at the University of East Anglia (UEA-200). Samples were spun at 3.65 kHz in a Bruker 7-mm double-bearing probe. Chemical shifts were externally referenced to adamantane [$\delta(^{13}C)$ = 37.7 relative to TMS]. $Zn(SAr'')_2$ (**1**) was prepared from Ar''SH and $Zn[N(SiMe_3)_2]_2$ as described previously.[3] Excess Ar''SH was removed by sublimation at 150 °C/0.01 mmHg.

X-ray Crystallography. X-ray measurements were made using an Enraf-Nonius FAST TV area detector diffractometer and graphite-monochromated Mo Kα radiation [λ(Mo Kα) = 0.710 69 Å] by following procedures previously outlined.[11] Colorless crystals of **1** were grown by

(1) (a) Dance, I. G. *Polyhedron* **1986**, *5*, 1037. (b) Blower, P. J.; Dilworth, J. R. *Coord. Chem. Rev.* **1987**, *76*, 121. (c) Canty, A. J.; Kishimoto, R.; Deacon, G. B.; Farquharson, G. J. *Inorg. Chim. Acta* **1976**, *20*, 161. (d) Dance, I. G. *J. Am. Chem. Soc.* **1980**, *102*, 3445. (e) Said, F. F.; Tuck, D. G. *Inorg. Chim. Acta* **1982**, *59*, 1. (f) Craig, D.; Dance, I. G.; Garbutt, R. G. *Angew. Chem.* **1986**, *98*, 178; *Angew. Chem., Int. Ed. Engl.* **1986**, *25*, 165. (g) Dance, I. G.; Garbutt, R. G.; Craig, D. C.; Scudder, M. L. *Inorg. Chem.* **1987**, *26*, 4057. (h) Dance, I. G.; Garbutt, R. G.; Craig, D. C.; Scudder, M. L.; Bailey, T. D. *J. Chem. Soc., Chem. Commun.* **1987**, 1164. (i) Dance, I. G.; Garbutt, R. G.; Scudder, M. L. *Inorg. Chem.* **1990**, *29*, 1571.

(2) Bochmann, M.; Webb, K.; Harman, M.; Hursthouse, M. B. *Angew. Chem.* **1990**, *102*, 703; *Angew. Chem., Int. Ed. Engl.* **1990**, *29*, 638.

(3) Bochmann, M.; Webb, K. J.; Hursthouse, M. B.; Mazid, M. *J. Chem. Soc., Dalton Trans.* **1991**, 2317.

(4) Bochmann, M.; Webb, K. J.; Coleman, A. P.; Hursthouse, M. B.; Mazid, M. *Angew. Chem.* **1991**, *103*, 975; *Angew. Chem., Int. Ed. Engl.* **1991**, *30*, 973.

(5) Bochmann, M.; Webb, K. J. *Mater. Res. Soc. Symp. Proc.* **1991**, *204*, 149.

(6) Bochmann, M.; Webb, K. J. *J. Chem. Soc., Dalton Trans.* **1991**, 2325.

(7) Huheey, J. E. *Inorganic Chemistry*; Harper & Row: New York, 1972; p 184.

(8) Power, P. P.; Shoner, S. C. *Angew. Chem.* **1990**, *102*, 1484; *Angew. Chem., Int. Ed. Engl.* **1990**, *29*, 1403.

(9) Bochmann, M.; Webb, K. J.; Hursthouse, M. B.; Mazid, M. *J. Chem. Soc., Chem. Commun.* **1991**, 1735.

(10) (a) Gruff, E. S.; Koch, S. A. *J. Am. Chem. Soc.* **1989**, *111*, 8762. (b) Gruff, E. S.; Koch, S. A. *J. Am. Chem. Soc.* **1990**, *112*, 1245.

(11) Danopoulos, A. A.; Wilkinson, G.; Hussain-Bates, B.; Hursthouse, M. B. *J. Chem. Soc., Dalton Trans.* **1991**, 1855.

0020-1669/93/1332-0532$04.00/0

Table I. X-ray Crystallographic Parameters for **1**

formula	$C_{72}H_{116}S_4Zn_2$
fw	1204.76
T, K	293
cryst system	triclinic
a, Å	10.333(5)
b, Å	11.226(9)
c, Å	32.266(30)
α, deg	81.29(2)
β, deg	86.12(2)
γ, deg	86.07(2)
V, Å^3	3684.70
Z	2
space group	$P\bar{1}$
d(calc), g cm^{-3}	1.118
radiation	Mo Kα
μ, cm^{-1}	8.05
θ range, deg	$1.5 \leq \theta \leq 27.0$
no. of reflcns measd	21 681
no. of unique reflcns with $\|F_o\| > 2\sigma\|F_o\|$	14 894
R_{int}	0.052
no. of obs reflcns	4519
no. of variables	796
$R = \sum\|\Delta F\|/\sum\|F_o\|$	0.059
$R_w = (\sum w\|F\|^2/\sum wF_o^2)^{1/2}$	0.068

sublimation at 200 °C at 0.01 mmHg as small blocks. A crystal of dimensions 0.2 × 0.22 × 0.18 mm^3 was used. Unit cell parameters and intensity data were obtained using the relevant procedures in the "small-molecule" version of the SADONL software.[12] The structure was solved via direct methods, developed via difference syntheses, and refined by blocked full-matrix least-squares techniques. The aryl rings were refined as idealized hexagons to reduce the number of parameters. Hydrogens were included in idealized positions and allowed to ride on the parent atoms. Intensity data were corrected for absorptions using the DIFABS method,[13] and unit weights were used, which gave satisfactory agreement analyses. The low number of observed data is a reflection of the poor diffracting power of the crystals of this kind of material. Crystallographic parameters are collected in Table I. Fractional atomic coordinates are given in Table II and have been deposited with the Director of the Cambridge Crystallographic Data Centre, University Chemical Laboratory, Lensfield Road, Cambridge CB2 1EW, U.K. Selected bond lengths and angles are given in Table III.

EHMO Calculations. The molecular orbital calculations were carried out within the framework of the extended Hückel approximation[14] using the parameters in Table IV. H_{ij} values were calculated by means of the modified Wolfsberg-Helmholtz approximation.[15] Population analysis followed the procedure described by Mulliken.[16]

Results and Discussion

NMR Studies. Within the series of complexes $Zn(SAr'')_2$ (**1**), $Zn(SeAr'')_2$ (**2**), $[Cd(SAr'')_2]_2$ (**3**), and $[Cd(SeAr'')_2]_2$ (**4**), it could be argued on steric grounds that compound **1** is most likely to possess a monomeric structure. Cryoscopic molecular weight determinations in benzene are not conclusive and suggest degrees of association of ca. 1.4 for **1** and 1.2–1.3 for **2**, i.e. the existence of monomers and dimers in solution. On the other hand, the very simple ^{1}H and ^{13}C NMR spectra of **1** in chloroform or toluene solutions at room temperature show the presence of only one ligand type and do not permit the distinction between terminal and bridging ligands. Low-temperature ^{1}H NMR spectra are consistent with rapid ligand exchange. The behavior of the signal for the aromatic meta protons at 7.25 ppm (singlet at 298 K) is characteristic for a two-site exchange process; the singlet broadens on cooling to 233 K, reaches coalescence at 228 K, and splits into two singlets at 7.17 and 7.33 on further cooling [$\Delta G^* \approx 10.9$ kcal mol^{-1} (228 K)]. In toluene-d_8, only signal broadening is seen and the low-exchange limit is not reached. The behavior of the aromatic C–H signals is mirrored by the signals for the ortho and para *tert*-butyl groups, although the temperature dependence is more complex. In dichloromethane solution, the signal of the para *tert*-butyl substituents begins to resolve into two components at $\delta = 1.28$ and 1.32 below 218 K. A similar splitting of the ortho *tert*-butyl groups is not observed until 208 K, followed by a reduction of line width on cooling to 193 K before hindered rotation of the C–S bonds of the thiolato ligands induces further broadening of the ortho *tert*-butyl groups at 183 K. This effect is more pronounced in toluene-d_8 solution, where the solvent induces larger chemical shift differences of the ortho *tert*-butyl signals. Again, the exchange of terminal and bridging Ar''S ligands is slow below 228 K, and the exchange between "inside" and "outside" ortho *tert*-butyl groups is slow enough to allow signal coalescence to be reached at ca. 183 K (Scheme I). The data do not allow us to distinguish unequivocally between a bimolecular and a unimolecular exchange mechanism (Scheme II), although the bimolecular mechanism is supported by the extensive dissociation into monomeric units revealed by molecular weight measurements.

The solid-state ^{13}C CP-MAS NMR spectra of **1**, **2**, and the crystallographically characterized dimer **3** show closely related structures for all three compounds. The complexes give surprisingly well defined solid-state NMR spectra at room temperature, with a resolution better than 0.5 ppm. Figure 1 illustrates the region of aromatic carbons (160–120 ppm) for **1**–**3**. The chemical shift data are given in Table V. The spectra of **2** and **3** are very similar and show two clearly resolved signals each for the ortho, meta, and para carbons and for *C*–S and *C*–Se, respectively, as expected for complexes with equal numbers of bridging and terminal chalcogenolato ligands, and confirm that **2** is structurally closely related to **3**. The spectrum of **1** is similar to those of **2** and **3** in its main features and clearly not that of a two-coordinate monomer; it shows however a larger number of signals for each type of carbon and points to a less symmetrical structure. This is in agreement with a centrosymmetric structure found for the molecule of **3** ($P2_1/n$), whereas in **1** the molecule occupies a general position in the crystal and possesses a more distorted structure, with six different Zn–S distances (see below). The spectra demonstrate that for molecules such as **1** solid-state ^{13}C NMR spectroscopy can provide a very quick and ready method to resolve structural ambiguities.

Crystal Structure of $Zn(SAr'')_2$ (1). While attempts to grow crystals from various solvents were unsuccessful, slow sublimation of **1** at 200 °C under reduced pressure gave small colorless plates suitable for X-ray diffraction. The molecule is a dimer (Figure 2), with three-coordinate zinc bonded to one terminal and two bridging sulfur ligands in a distorted trigonal-planar geometry; the angle sums for zinc are 359.5 for Zn(1) and 357.9° for Zn(2). The Zn_2S_2 ring forms an almost planar parallelogram reminiscent of the structure of **3**[2] and its selenium analogue **4**;[3] individual atom deviations are all 0.05(2) Å, giving a slight fold along the S(1)–S(2) vector of 8.6(1)°. The thiolate bridges are distinctly asymmetric, average Zn–S distances being 2.281(5) and 2.400(5) Å. The terminal Zn–S bonds are very short, 2.194(5) Å on average, i.e. 0.087 and 0.206 Å shorter than the bridging distances. This bond length is significantly shorter than the sum of the ionic radii for Zn and S, 2.56 Å[7]. The bond length distribution in **1** closely reflects the bonding situation in the cadmium complexes **3** and **4**. Similar terminal Zn–S distances are found in $Zn(SAr'')_2(Et_2O)$ (average 2.195 Å),[8] whereas nonbridging Zn–S bond lengths in four-coordinate complexes range from ca. 2.25 to 2.35 Å.[10,17] Although there is considerable variation in Zn–S bond lengths, a comparison of a number of structurally characterized

(12) Pflugrath, J. W.; Messerschmidt, A. *The MADNES System*, version 11.9 (1989), modified for small-molecule work by B. Schierbeck, Enraf-Nonius, Delft, The Netherlands.
(13) Walker, N.; Stuart, D. *Acta Crystallogr., Sect. A* **1989**, *39*, 158.
(14) Hoffmann, R. *J. Chem. Phys.* **1963**, *39*, 1397.
(15) Ammeter, J. H.; Bürgi, H. B.; Thibeault, J. C.; Hoffmann, R. *J. Am. Chem. Soc.* **1978**, *100*, 3686.
(16) Mulliken, R. S. *J. Chem. Phys.* **1955**, *23*, 1833.
(17) (a) Cremers, T. L.; Bloomquist, D. R.; Willet, R. D.; Crosby, G. A. *Acta Crystallogr., Sect. B* **1980**, *36*, 3097. (b) Corwin, D. T.; Koch, S. A. *Inorg. Chem.* **1988**, *27*, 493. (c) Ueyama, N.; Sugawara, T.; Sasaki, K.; Nakamura, A.; Yamashita, S.; Wakatsuki, Y.; Yamazaki, H.; Yasuoka, N. *Inorg. Chem.* **1988**, *27*, 741.

Table II. Fractional Atomic Coordinates (×10⁴) and Equivalent Isotropic Temperature Factors (Å² × 10³) for **1**

	x	y	z	U_{eq}[a]		x	y	z	U_{eq}[a]
Zn(1)	1143(1)	1628(1)	2321.1(4)	36(1)	C(58)	−3118(5)	4222(4)	4155(1)	37(2)
Zn(2)	179(1)	3689(1)	3000.0(4)	35(1)	C(59)	−1828(5)	4375(4)	4011(1)	30(2)
S(1)	530(3)	1651(2)	3042(1)	32(1)	C(60)	−1540(5)	5167(4)	3645(1)	24(2)
S(2)	584(3)	3651(2)	2252(1)	33(1)	C(61)	−2344(10)	6848(8)	3041(3)	36(2)
S(3)	2008(3)	−12(3)	2102(1)	51(1)	C(62)	−1982(11)	6315(9)	2634(3)	47(2)
S(4)	90(3)	5137(2)	3394(1)	34(1)	C(63)	−1332(12)	7725(10)	3115(4)	58(3)
C(1)	−1838(5)	856(4)	3423(2)	26(2)	C(64)	−3593(12)	7660(10)	2960(4)	63(3)
C(2)	−2572(5)	259(4)	3760(2)	34(2)	C(65)	−5556(9)	4607(10)	4069(3)	42(3)
C(3)	−1956(5)	−517(4)	4076(2)	31(3)	C(66)	−6446(13)	4913(20)	3729(5)	172(3)
C(4)	−605(5)	−697(4)	4055(2)	34(3)	C(19)	2652(5)	4993(5)	1873(2)	37(2)
C(5)	130(5)	−101(4)	3717(2)	32(2)	C(20)	3357(5)	5565(5)	1524(2)	45(3)
C(6)	−487(5)	676(4)	3402(2)	23(2)	C(21)	2841(5)	5731(5)	1130(2)	43(3)
C(7)	−2677(9)	1593(8)	3061(3)	30(2)	C(22)	1619(5)	5324(5)	1084(2)	42(2)
C(8)	−2659(10)	2964(9)	3062(4)	46(2)	C(23)	915(5)	4752(5)	1433(2)	31(2)
C(9)	−4129(10)	1299(10)	3138(4)	55(3)	C(24)	1431(5)	3586(5)	1828(2)	26(2)
C(10)	−2251(12)	1279(10)	2626(3)	54(2)	C(25)	3266(10)	5052(11)	2300(3)	47(3)
C(11)	−2744(10)	−1118(10)	4467(3)	44(2)	C(26)	2371(11)	5896(10)	2555(3)	52(3)
C(12)	−4140(15)	−867(18)	4444(6)	169(3)	C(27)	3505(12)	3824(11)	2570(4)	65(3)
C(13)	−2340(18)	−772(18)	4857(4)	150(3)	C(28)	4597(12)	5594(15)	2245(5)	100(3)
C(14)	−2455(18)	−2469(14)	4504(6)	151(3)	C(29)	3658(13)	6333(12)	745(4)	67(3)
C(15)	1637(10)	−482(9)	3709(3)	41(2)	C(30)	4072(19)	7477(15)	807(5)	159(3)
C(16)	2456(11)	561(11)	3775(4)	66(3)	C(31)	2980(18)	6477(17)	340(5)	149(3)
C(17)	2115(11)	−939(10)	3292(4)	59(3)	C(32)	4812(16)	5479(16)	663(5)	137(3)
C(18)	1980(12)	−1519(13)	4052(4)	84(3)	C(33)	−504(10)	4407(9)	1344(3)	40(2)
C(43)	4491(12)	951(12)	1501(4)	67(3)	C(34)	−1548(11)	4947(10)	1631(4)	58(3)
C(44)	5001(13)	−260(13)	1722(5)	95(3)	C(35)	−868(13)	4938(12)	894(4)	72(3)
C(45)	5550(13)	1319(16)	1158(5)	110(3)	C(36)	−572(12)	3038(10)	1388(4)	63(2)
C(46)	4404(14)	1913(14)	1799(5)	100(3)	C(37)	3142(5)	840(6)	1314(2)	47(3)
C(47)	1895(13)	1635(12)	207(4)	67(3)	C(38)	3092(5)	1255(6)	885(2)	56(3)
C(48)	515(14)	1825(15)	64(4)	107(3)	C(39)	2013(5)	1058(6)	673(2)	47(2)
C(49)	2460(18)	2881(15)	119(5)	144(3)	C(40)	983(5)	447(6)	889(2)	42(3)
C(50)	2646(19)	866(18)	−58(5)	158(3)	C(41)	1032(5)	32(6)	1318(2)	34(2)
C(51)	−61(10)	−840(9)	1511(3)	41(2)	C(42)	2112(5)	229(6)	1531(2)	39(2)
C(52)	−885(12)	−1187(11)	1174(4)	73(3)	C(67)	−5952(14)	5165(17)	4433(5)	128(3)
C(53)	560(12)	−2057(10)	1720(4)	57(3)	C(68)	−5717(15)	3266(15)	4207(7)	171(3)
C(54)	−989(11)	−294(10)	1822(4)	59(2)	C(69)	−775(9)	3770(9)	4325(3)	35(2)
C(55)	−2543(5)	5806(4)	3422(1)	26(2)	C(70)	118(10)	4694(11)	4422(4)	57(3)
C(56)	−3833(5)	5653(4)	3566(1)	32(2)	C(71)	−17(11)	2714(11)	4148(4)	64(2)
C(57)	−4121(5)	4861(4)	3932(1)	38(2)	C(72)	−1401(11)	3263(12)	4751(3)	60(2)

[a] U_{eq} is defined as one-third of the trace of the orthogonalized U_{ij} tensor.

Table III. Selected Bond Lengths (Å) and Angles (deg) for **1**

Zn(2)–Zn(1)	3.473(5)	S(1)–Zn(1)	2.371(5)
S(2)–Zn(1)	2.285(5)	S(3)–Zn(1)	2.184(5)
S(1)–Zn(2)	2.277(5)	S(2)–Zn(2)	2.429(5)
S(4)–Zn(2)	2.203(5)	C(6)–S(1)	1.805(7)
C(24)–S(2)	1.808(8)	C(42)–S(3)	1.821(8)
C(60)–S(4)	1.819(8)		
S(2)–Zn(1)–S(1)	84.5(2)	S(3)–Zn(1)–S(2)	154.2(1)
S(3)–Zn(1)–S(1)	120.8(2)	S(4)–Zn(2)–S(2)	133.4(1)
S(2)–Zn(2)–S(1)	83.4(2)	C(6)–S(1)–Zn(1)	130.6(2)
S(4)–Zn(2)–S(1)	141.1(1)	Zn(2)–S(2)–Zn(1)	94.9(2)
Zn(2)–S(1)–Zn(1)	96.7(2)	C(24)–S(2)–Zn(2)	134.8(2)
C(6)–S(1)–Zn(2)	119.3(3)	C(42)–S(3)–Zn(1)	108.7(3)
C(24)–S(2)–Zn(1)	116.0(3)	C(60)–S(4)–Zn(2)	106.0(3)

Table IV. Parameters Used in EHMO Calculations

atom	orbital	H_{ii}, eV	ζ_1	ζ_2	C_1[a]	C_2[a]
H	1s	−13.60	1.30			
S	3s	−20.00	2.12			
	3p	−11.00	1.83			
Zn	3d	−15.70	6.15	2.40	0.5437	0.6204
	4s	−10.55	2.30			
	4p	−6.30	2.30			

[a] Coefficients in the double-ζ expansion.

complexes (Table VI) shows that, as a general rule, terminal Zn–S distances of three-coordinate compounds are ca. 0.06–0.1 Å shorter than those of comparable four-coordinate analogues. A similar bond shortening on reducing the coordination number from 4 to 3 has been observed for alkoxides and thiolates of Al and Ga.[21,22] On the other hand, the Zn–S distances of bridging thiolato ligands do not allow such a distinction, and the bond

Scheme I

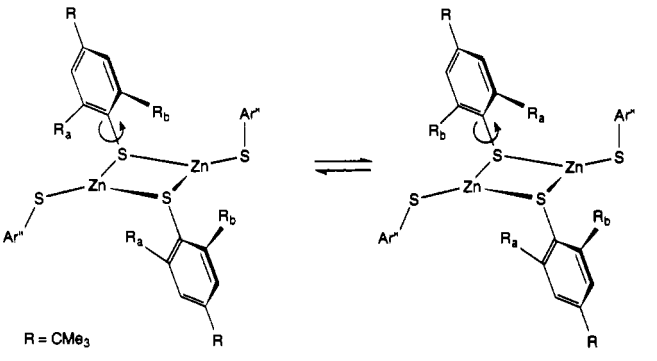

lengths of three- and four-coordinate zinc complexes fall within very similar ranges.[18-20]

Whereas Zn is trigonal-planar, the bridging sulfur atoms are pyramidal, with angle sums of 346.6° [S(1)] and 345.7° [S(2)]. Similar angles around sulfur have previously been found in the trimeric compounds $[Me_3SiCH_2Zn(SC_6H_2R_3)]_3$ (R = *i*-Pr, *t*-Bu), for which a degree of electron delocalization throughout the ring

(18) Olmstead, M. M.; Power, P. P.; Shoner, S. C. *J. Am. Chem. Soc.* **1991**, *113*, 3379.
(19) Kaptein, B.; Wang-Griffin, L.; Barf, G.; Kellogg, R. M. *J. Chem. Soc., Chem. Commun.* **1987**, 1457.
(20) Hursthouse, M. B.; Malik, M. A.; Motevalli, M.; O'Brien, P. *Organometallics* **1991**, *10*, 730.
(21) (a) Shreve, A. P.; Mulhaupt, R.; Fultz, W.; Calabrese, J.; Robbins, W.; Ittel, S. D. *Organometallics* **1988**, *7*, 409. (b) Petrie, M. A.; Olmstead, M. M.; Power, P. P. *J. Am. Chem. Soc.* **1991**, *113*, 8704.
(22) Ruhlandt-Senge, K.; Power, P. P. *Inorg. Chem.* **1991**, *30*, 2633, 3683.

Scheme II

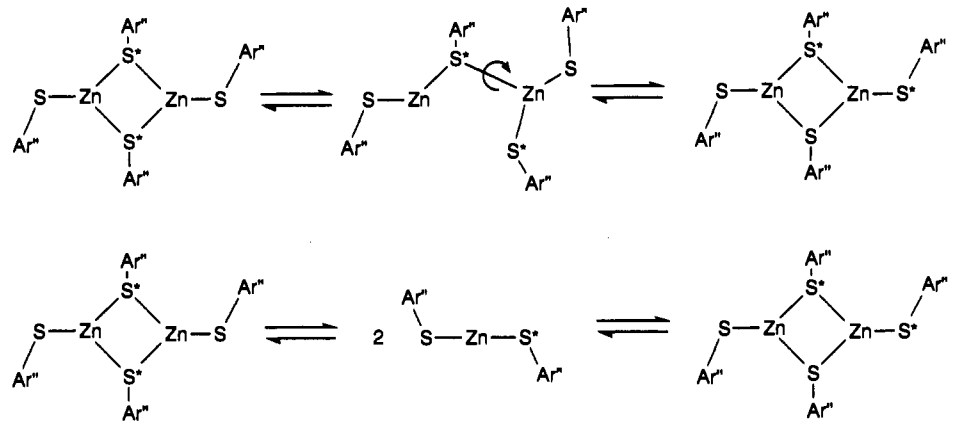

Table V. ^{13}C CP-MAS NMR Data for $Zn(SAr'')_2$, $Zn(SeAr'')_2$, and $Cd(SAr'')_2$[a]

$Zn(SAr'')_2$ (1)	$Zn(SeAr'')_2$ (2)	$Cd(SAr'')_2$ (3)	assgnt
153.9	153.2	153.6	
153.3	152.6	151.5	*o*-C
152.7	151.7		
151.5			
148.8 br	148.4	147.8	*p*-C
147.3	146.9	146.3	
145.1			
129.7 br	124.1	130.8	E-C
127.5	120.5	128.4	E-C
126.9			
123.9			
122.1	122.9	121.7 s, br	*m*-C
121.2	121.7	120.5	
120.3			

[a] At 50.29 MHz; spinning rate 3.65 kHz.

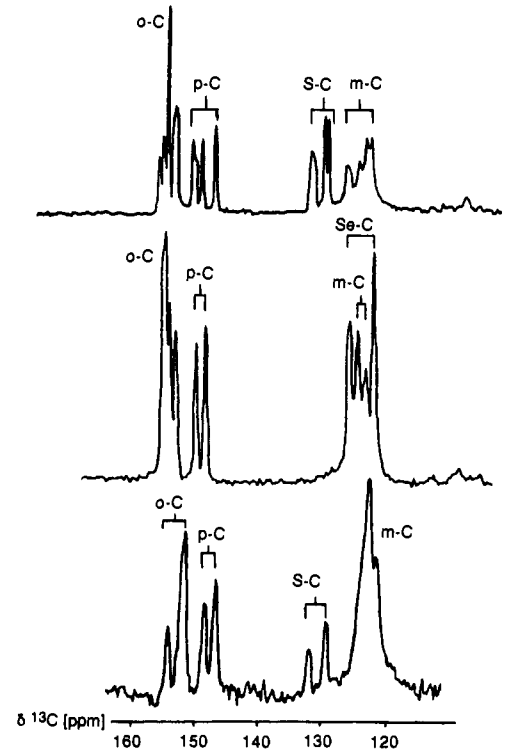

Figure 1. CP-MAS ^{13}C NMR spectra of the aromatic region of $Zn(SAr'')_2$ (1), $Zn(SeAr'')_2$ (2), and $Cd(SAr'')_2$ (3). Spinning rate: 3.65 kHz.

has been discussed,[18] and for the dimeric transition metal thiolates $[M(SAr'')_2]_2$, where the pyramidality of S increases from 340.3 to 313.2° in the series M = Mn < Fe < Co.[23] By contrast, the

Table VI. Comparison of the Terminal and Bridging Bond Distances in Zinc Thiolato Complexes

complex	coord no.	*r*(Zn–S), Å terminal	*r*(Zn–S), Å bridging	ref
1	3	2.194[a]	2.281, 2.400[a]	this work
$Zn(SAr'')_2(Et_2O)$	3	2.196[a]		8
$Zn(SAr')_2(bipy)$[b]	4	2.255[a]		17b
$Zn(SC_6HMe_4)_2(imid)_2$	4	2.300		17b
$[Zn(SC_6HMe_4)_3]^-$	3	2.230[a]		10a
$[Zn(SC_6HMe_4)_3(imid)]^-$	4	2.326[a]		10a
$[Zn(SPh)_4]^{2-}$	4	2.357		17c
$[RZn(SCPh_3)]_2$[c]	3		2.381, 2.416	18
$[RZn(SAr')]_3$[b,c]	3		2.289–2.327	18
$[RZn(SAr'')]_3$[c]	3		2.291–2.372	18
$Zn_4(SPh)_8(MeOH)$	4		2.342[a]	1d
$[ZnC_5H_3N(CH_2CPh_2S)_2]_2$	4		2.350, 2.425	19
$[MeZn(S_2CNEt_2)]_2$	4	2.370	2.501, 2.512	20

[a] Average value. [b] Ar' = 2,4,6-*i*-$Pr_3C_6H_2$. [c] R = CH_2SiMe_3.

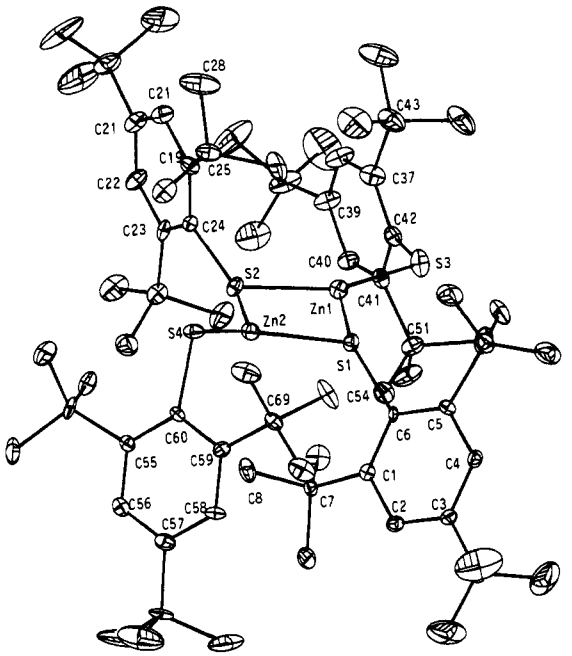

Figure 2. Molecular structure of **1**, showing the atomic numbering scheme. Thermal ellipsoids are drawn at 30% probability.

sulfur bond angles in related dimeric zinc thiolates such as $[Me_3SiCH_2Zn(SCPh_3)]_2$ are considerably more acute (angle sum 285.6°),[18] and it appears that there is sufficient flexibility in these compounds to accommodate a large variation of steric requirements.

(23) Power, P. P.; Shoner, S. C. *Angew. Chem.* **1991**, *103*, 308; *Angew. Chem., Int. Ed. Engl.* **1991**, *30*, 330.

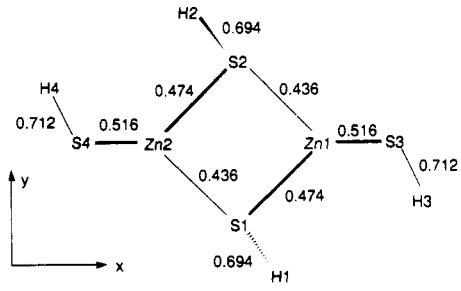

Figure 3. Idealized geometry of $[Zn(SH)_2]_2$ for EHMO calculations, showing the atom–atom bond population densities, with H(1) and H(2) approximately in the crystallographic positions of carbons C(24) and C(6), respectively, in the structure of **1**. Stronger bonds are indicated by thick lines.

The aryl substituents of the bridging ligands are not strictly perpendicular to the Zn_2S_2 plane; the dihedral angle of ring C(1)–C(6) with the Zn(1)–S(1)–Zn(2) plane is 70.5(1)°, while the second ring C(19)–C(24) gives an angle of 98.8(1)° with plane Zn(1)–S(2)–Zn(2). The spaces above and below the zinc atoms are occupied by methyl groups of the *tert*-butyl substituents from both bridging *and* terminal aryl groups, with Zn–C distances ranging from 3.08 Å [C(8)–Zn(2)] to 3.78 Å [C(54)–Zn(1)]. Some Zn–aryl-C distances fall into this range also (see supplementary material). Since the methyl hydrogen atoms were not located experimentally, no firm indication can be given about possible Zn–H interactions.

The Zn–S–C angles of the terminal ligands are unexceptional, 106 and 108.7°. The ligands adopt orientations so as to minimize steric interactions with the bridging groups, with torsion angles of the planes C(60)–S(4)–Zn(2) and C(42)–S(3)–Zn(1) with respect to the Zn_2S_2 plane of 70.56 and 13.59°, respectively. Steric interactions are presumably also responsible for the large variation of angles around the zinc centers; for example, the bond vector Zn(1)–S(3) forms angles of 154.2 and 120.8° with Zn(1)–S(2) and Zn(1)–S(1), respectively; both deviate significantly from a "symmetrical" arrangement for which exocyclic angles of 137.5° might be expected. The angles around Zn(2) vary less, 133.4 and 141.1°. In both cases, the more acute angles are formed between the terminal and the longer of the bridging bonds.

Bonding Considerations and EHMO Calculations. The asymmetry of the thiolate bridges in **1** is striking and requires an explanation. Since the same structural feature is found also in the Cd–S and Cd–Se complexes **3** and **4**, i.e. in compounds with significantly different atomic radii, the cause is unlikely to be steric congestion in **1**. On the other hand, zinc–sulfur bonds are highly covalent, as measured by the Allred–Rochow electronegativity difference of only 0.78, and zinc(II) has vacant p orbitals suitable for overlap with a nonbonding electron pair on sulfur, so that a superficial explanation might invoke a $(p–p)_\pi$ interaction between zinc and sulfur involving four electrons, which would lead to a Hückel antiaromatic bonding in the Zn_2S_2 ring, with a consequent cyclobutadiene-like distortion:

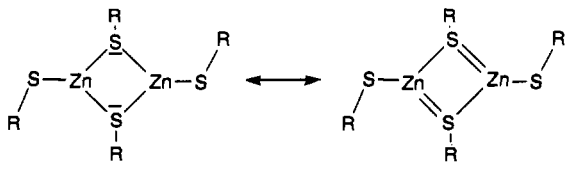

However, the high inversion barrier of sulfur makes such extensive π-interaction very unlikely, and although it has been argued that some charge delocalization may be present in Zn_3S_3 rings,[18] π-bonding with second-row elements such as sulfur should be treated with caution.

We have attempted to shed light on the bonding situation with extended Hückel molecular orbital calculations on $Zn_2(\mu\text{-}SH)_2$-$(SH)_2$ as a simplified model with an idealized geometry. The sulfur-bonded carbons were modeled by hydrogens constrained to positions close to those found experimentally for **1**, with a S–H distance of 1.35 Å. All Zn–S bond lengths were kept at identical lengths and set at 2.290 Å, the average Zn–S distance of **1**. The calculated atom–atom populations (Figure 3) are a measure of the relative Zn–S bond strengths and show the existence in the Zn_2S_2 ring of two types of Zn–S bonds of different strength, both of which are weaker than the terminal Zn–S bond; this reflects the experimental findings. The charge density distribution confirms the highly covalent character of the molecule: the zinc atoms accumulate a charge of ca. +0.4, the bridging sulfur atoms are essentially uncharged, and the terminal sulfurs carry a charge of –0.4 each.

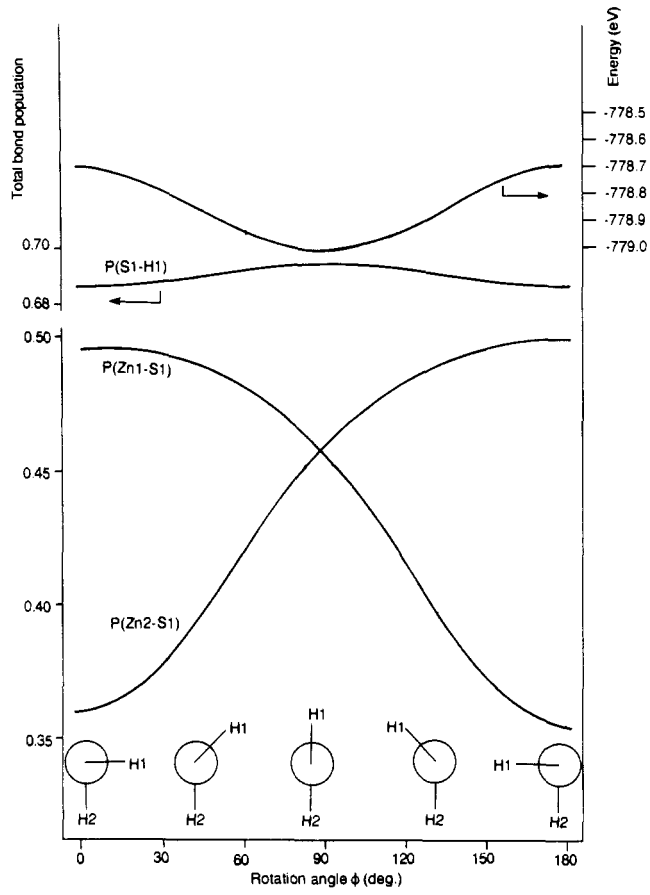

Figure 4. Dependence of the Zn–S skeletal bond populations of the Zn_2S_2 ring and of total energy (eV) on the rotational angle of the S(1)–H(1) bond.

For the terminal bonds Zn(1)–S(3) and Zn(2)–S(4), by far the largest bonding contribution is due to the overlap of the sulfur p_x orbital with the zinc s and p_x orbitals, with minor contributions (ca. 20%) from the sulfur s orbital. Any bonding contribution due to π-type interaction of p_z orbitals is negligible (≈5%); the strength of the bond is a consequence of the favorable orientation of the participating orbitals along the x axis.

There is no electronic reason that the substituents H(1) and H(2) of the bridging thiolato ligands should be moved out of the yz plane toward the positions found for C(6) and C(24) in **1**. In the absence of steric interaction, the minimum of total energy is at the 90° position, i.e. with H(1) and H(2) in the yz plane and in trans positions relative to each other, although the energy trough is fairly shallow (Figure 4). In this case, the populations of all four bridging bonds are essentially identical, apart from very small differences due to the positions of H(3) and H(4) off the x axis. This situation is typical of the symmetrical bridges of smaller chalcogenolato ligands where steric hindrance is moderate (cf. $[Cd(TeC_6H_2Me_3)_2]_n$[4]). The thiolato bridges are mainly due

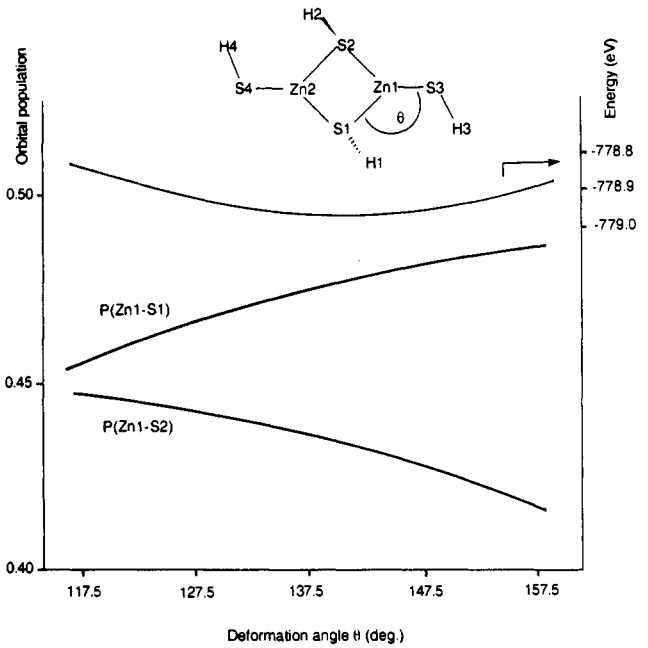

Figure 5. Zn–S ring bond populations and total energy as a function of the deformation angle θ.

to overlap of S-s and S-p_x with Zn-s, Zn-p_y, and, to a lesser extent, Zn-p_x orbitals. The interaction of sulfur p_y with the zinc orbitals contributes only ca. 20–30% of the total population; however, this bonding contribution is remarkably sensitive to the position of the associated hydrogen atoms H(1) and H(2). If H(1) is rotated out of the *yz* plane, e.g. toward Zn(1), bond Zn(1)–S(1) is strengthened while Zn(2)–S(1) becomes correspondingly weaker, almost exclusively as the result of changes in overlap between the sulfur p_y and the zinc s, p_x, and p_y orbitals. The S(1)–H(1) bond is essentially insensitive to the S–H rotation. Figure 4 illustrates this trend for the changes in total populations of the Zn(1)–S(1) and Zn(2)–S(1) bonds as a function of the rotation of H(1); the angle of the S(1)–H(1) vector with the S(1)–S(2) axis remains at 31.3° throughout. The population differences are sufficient to account for the observed bond length alternation within the Zn_2S_2 ring of **1**. Again, π contributions to bonding in the Zn_2S_2 ring are negligible (<6%), as is the contribution of zinc d orbitals, which are slightly antibonding in character.

The calculations represented in Figure 4 were carried out by assuming an idealized geometry where the terminal sulfurs, S(3) and S(4), are positioned on the *x* axis, with angles S_{term}–Zn–S_{br} of 137.5°. While for S(4) this corresponds closely to the crystallographically determined angles of 141.1(1) and 133.4(1)°, for S(3) the structure of **1** shows significant deviations from the mean, with values of 120.8(2) and 154.2(1)°. The effect on the total population density of bonds Zn(1)–S(1) and Zn(1)–S(2) was probed accordingly by varying the deformation angle θ from 117.5 to 157.5° (137.5 ± 20°) (Figure 5). Although the changes in the ring bond populations are comparatively minor, they do reinforce the inequality of the electron densities of the bridging bonds of **1**. The origin of the displacement of the bridging aryl substituents out of the *yz* plane, and thereby of the asymmetry of the thiolate bridges, is very likely steric. The resulting changes in the electronic structure of **1** were somewhat unexpected but are apparently not confined to complexes **1**, **3**, and **4**. A comparison with related dimeric alkoxo and thiolato structures, such as $[RZnEX]_2$ (E = O, X = C_6H_2-*i*-Pr_3; C_6H_2-*t*-Bu_3; E = S, X = CPh_3)[18] confirms qualitatively that bond length variations in the M_2E_2 rings are related to M–E–X angle variations. Interestingly, such distortions are essentially absent in complexes with partially filled d shells, such as $[M(SAr'')_2]_2$ (M = Mn, Fe, Co).[23]

Conclusion

The sterically highly hindered arene thiolato ligand Ar''S^- forms a volatile zinc complex $[Zn(SAr'')_2]_2$ (**1**), which is dimeric in the solid state, with three-coordinate zinc. The behavior in hydrocarbon solution suggests dissociation into monomeric two-coordinate species and facile ligand exchange, although a dimeric structure is present in solution at low temperatures. The thiolato bridges in crystalline **1** are asymmetric; EHMO calculations suggest that the origin of this asymmetry lies in a sterically induced displacement of the sulfur-bound aryl substituents, which induces subtle changes in the bond populations of the Zn_2S_2 skeleton. The shortness of the terminal Zn–S bonds is a consequence of efficient orbital overlap and of the low metal coordination number; there is no requirement to invoke zinc–sulfur p_π–p_π interactions to explain the bonding pattern in chalcogenolato dimers such as **1**.

Acknowledgment. This work was supported by the U.K. Science and Engineering Research Council and the Royal Signals and Radar Establishment. We are grateful to Professor R. Hoffmann for a helpful communication.

Supplementary Material Available: Tables giving bond lengths, bond angles, thermal parameters, H atom coordinates, and nonbonding distances (16 pages). Ordering information is given on any current masthead page.